J Am Oil Chem Soc (2010) 87:681–688
DOI 10.1007/s11746-010-1542-9

ORIGINAL PAPER

Synthesis and Characterization of the Intrinsic Properties of Milkweed Polyhydroxy Fatty Acids

R. E. Harry-O'kuru · A. Mohamed · S. H. Gordon · J. Xu · B. K. Sharma

Received: 5 August 2009 / Revised: 12 November 2009 / Accepted: 31 December 2009 / Published online: 3 February 2010

Abstract Seed oils consist mainly of triglycerides, that is, they comprise a unit of glycerol backbone esterified with three acyl groups (usually but not limited to C16–C18) which may be saturated or unsaturated with one or more olefinic functionalities per acyl group. Very rarely do seed oils contain additional functional groups, such as hydroxyls as in castor and lesquerella seeds. Milkweed seed oil follows the natural triglyceride patterns, but with a difference in being highly poly olefinic. This character allows for the introduction of different reactive groupings into the structure of the oil so as to be amenable to tailoring to a variety of uses. Synthesis of the milkweed polyhydroxy triglyceride (MWPHTG) from the polyoxirane triglyceride derivative of milkweed oil using in situ peroxy acid epoxidation of the oil was previously reported. Subsequent acidolysis of the epoxy derivative gave the MWPHTG. Here the polyhydroxy triglyceride was saponified for glycerol removal thus generating the polyhydroxy fatty acids of milkweed oil. Studies of the physical characteristics, flow and stability of the resulting hydroxylated fatty acids using FTIR, NMR, DSC, Rheometry and TGA indicate a stable material with unique properties that would be useful as additives in many applications such as pharmaceuticals.

Keywords Milkweed oil · Polyhydroxy milkweed fatty acids · Differential scanning calorimetry · Pressure DSC · Oxidation kinetics · Rheometry · Viscoelastic properties

R. E. Harry-O'kuru (✉)
New Crops and Processing Technology Research Unit,
National Center for Agricultural Utilization Research,
United States Department of Agriculture,
Agricultural Research Service, 1815 N. University Street,
Peoria, IL 61604, USA
e-mail: Rogers.HarryOkuru@ars.usda.gov

A. Mohamed · S. H. Gordon · J. Xu
Cereal Products and Food Science Research Unit,
National Center for Agricultural Utilization Research,
United States Department of Agriculture,
Agricultural Research Service, 1815 N. University Street,
Peoria, IL 61604, USA

B. K. Sharma
Food and Industrial Oils Research Unit,
National Center for Agricultural Utilization Research,
United States Department of Agriculture,
Agricultural Research Service, 1815 N. University Street,
Peoria, IL 61604, USA

Introduction

The narrow range of functional groupings present in most seed oils, namely, the olefin and the ester in triglycerides, may initially seem to give the oils limited usefulness other than feed substrates. A second look, however, reveals these as natural platforms for tailoring of triglycerides into desired renewable substrates for the creation of multiple synthetic intermediates and end products. The common milkweed (*Asclepias syriaca* L.) is native in the Americas and its seed oil is very unsaturated (92%). Hydroxylation of the oil by functionalization of the olefinic groups introduces polar characteristics to an otherwise non-polar substrate and so broadens the utility and stability of this renewable resource [1]. The behavior of the induced polar environment within the triglyceride molecules can be further accentuated by removal of the esterifying glycerol moieties to generate polyhydroxy fatty acids. These could

serve many industrial applications including additives such as viscosity modifiers in foods, lubricants, pharmaceuticals and biodegradable plastics. This study explores the physical behavior of these novel acids vis-à-vis the known properties of triglycerides.

It is known that the kinetics and thermal properties of different synthetic polymers and biopolymers can be determined by differential scanning calorimetry (DSC). Ozawa [2] demonstrated that non-isothermal DSC data can be used to determine activation energy (E_a) presuming that the maximum reaction rate temperature is identical to the peak temperature (T_p) determined by DSC. The reaction rate for a solid product A to produce a solid product B can be expressed as follows:

$$\frac{dx}{dt} = Ze^{-E_a/RT}(1-x)^n \quad (1)$$

where x fraction reacted, Z pre-exponential factor, n reaction order, E_a activation energy, T absolute temperature, and R universal gas constant (8.314 J K^{-1} mol^{-1}). If the temperature of a first order reaction ($n = 1$) was raised constantly, the following equation makes possible the determination of the E_a of the material using DSC data as described by Mohamed et al. [3].

$$\ln\left(\frac{\beta}{T_p^2}\right) = \ln\left(\frac{RZ}{E_a}\right) - \left[\left(\frac{E_a}{R}\right)\left(\frac{1}{T_p}\right)\right] \quad (2)$$

where β constant rate of temperature rise, and T_p peak temperature. The natural logarithm transformation was used to linearize the equation. From Eq. 2, the plot of $1/T_p$ as a function of $-\ln(\beta/T_p^2)$ will represent a straight line with slope $= R/E_a$, thus the E_a value can be calculated ($E_a = R/\text{slope}$).

The thermogravimetric analysis (TGA) data were plotted as temperature versus wt% or temperature versus derivative of wt%, from which onset and final decomposition temperatures were obtained as well as the degradation kinetics. Different heating rates are usually used to calculate the E_a of degradation according to Flynn and Wall [4] based on the following equation

$$\log\beta \cong 0.457\left(-\frac{E_a}{RT}\right) + \left[\log\left(\frac{AE_a}{R}\right) - \log F(a) - 2.315\right] \quad (3)$$

where β, R and T are as above, a is the conversion and A is the pre-exponential factor. According to this equation, at the same percent conversion, E_a can be obtained from the slope of the plot of log β versus 1,000/T (K). The calculation of E_a was done using the software provided by TA Instruments (New Castle, DE, USA). The E_a value was determined for each sample at each heating rate in addition to the percent conversion per min reported.

Materials and Methods

Materials

Milkweed polyhydroxy triglycerides (MWPHTG) were from our in-house stock that had previously been synthesized from our supply of milkweed oil [1]. KOH pellets, HCl, ethyl acetate, 2-propanol, and sodium bicarbonate were purchased from Fisher Scientific (Chicago, IL, USA), acetic anhydride was purchased from ACRŌS Organics (Chicago, IL, USA) whereas pre-coated TLC plates (5 × 20 cm) were from EM Science (Darmstadt, Germany).

Methods

Synthesis of Milkweed Polyhydroxy Triglycerides

In a 1-L jacketed flask was placed reprocessed milkweed oil (648.0 g, 759.9 mmol). The oil was stirred vigorously at 40 °C and formic acid (90.4%, 62.2 g, 1.22 mol) was added in one portion followed with a slow (dropwise) addition of H_2O_2 (50%, 203.0 g, 2.98 mol). At the end of peroxide addition, the temperature was increased to 70 °C. After 15 h the heat source was removed but stirring was continued, allowing the reaction mixture to cool to room temperature and the aqueous phase removed. Deionized water (300 mL) was added followed with 6 M HCl (100 mL). The nearly colorless sludge was stirred at 70 °C overnight. The cream colored product was transferred into a separatory funnel using ethyl acetate as diluent. The aqueous layer was discarded and the organic phase washed sequentially with brine, saturated $NaHCO_3$ to pH 7.5 followed with deionized water. Ethanol was added to facilitate separation of the phases. After removal of the aqueous layer, the product was concentrated in vacuo at 70 °C to yield 711.6 g (94.7%) of the polyhydroxyl triglyceride with an oxirane value = 1.35; iodine value = 14 compared to an iodine value of 114 in the starting milkweed oil. The measured kinematic viscosities were: $\eta_{40\ °C} = 2332.5$ and $\eta_{100\ °C} = 75.53$ cSt, that is, a viscosity index of 85. Specific rotation $[\alpha]_D^{20} = +0.37$E. IR (film on NaCl) ν cm^{-1}: 3636–3168 b (O–H stretch), 2927 vs (–CH_3, –CH_2– asym stretch), 2856 vs (–CH_2, –CH_3 sym stretch), 1743 vs (–C=O stretch), 1463 s (–CH_2– deform), 1378 m-s (–CH_3 deform.), 1240 m-s (O=C–O–C stretch), 1173 vs (–CHO), 1097 s (CHO), 881 w, 725 w (–CH_2– wag). ^{13}C-NMR ($CDCl_3$) δ (ppm): 173.2, 172.8 (–C=O); 84.60, 83.00, 82.50, 82.00, 80.50, 74.40, 73.82, 73.20 (**C**HO); 68,82 (CHO glycerol backbone); 62.04 (–CH_2O– glycerol backbone); 34.75, 34.48, 34.10, 33.94, 33.54 (–$CH_2\alpha$– to carboxyl groups); 31.79, 31.61(–CH_2s– sandwiched between –CHOs–), 30.47, 29.64, 29.56, 29.47, 29.42, 29.31, 29.26,

29.21, 29.17, 29.05, 28.91, 25.58, 25.26, 24.76 (–CH_2–); 22.61, 22.56, 22.45 (–**C**H_2–CH_3; 14.08 (–**C**H_3).

Milkweed Polyhydroxy Fatty Acids

MWPHTG (21.0 g, 0.03188 mol), as previously reported above [1], was placed in a 250-mL jacketed reactor containing 2-propanol (35.0 mL). KOH pellets (87.7%, 5.0 g, 78.16 mmol) were added to the mixture which was then stirred and heated to 70 °C, allowing for gentle reflux. After 6 h of reflux, TLC of the reaction mixture on precoated silica gel plate using ethyl acetate: 2-propanol (2:1) as solvent indicated complete reaction. The product mixture was transferred into a beaker with 50 mL deionized water and the pH of the resulting solution adjusted to ~5.5 with 6 M HCl. The aqueous solution was then extracted with ethyl acetate (50 mL × 3); the extract was dried over $MgSO_4$ and concentrated at 57 °C under reduced pressure to give the MWPHFA (19.2 g, 95% of theoretical). The product initially an oil had $R_f = 0.63$ compared to $R_f = 0.75$ for the polyhydroxy triglyceride; it eventually solidified on standing. Its Fourier Transform Infrared (FTIR) spectrum on $NaCl_{film}$ ν cm^{-1}: 3395 br (OH stretch), 2925 vs (CH_3, CH_2 asym stretch), 2853 vs (CH_3, CH_2 sym stretch), 1714 s (–CO_2H stretch), 1558 m (CO_2^- stretch), 1465 m-s (–CH_2– deform.), 1377 m-s (–CH_3 deform), 1253 br (–OCO stretch), 1051 br (–CH_2O– stretch), 720 w (CH_2 wag); compared to the latter, the spectrum of the precursor triglyceride film on NaCl cm^{-1}: 3437 br (O–H stretch), 2927 vs (–CH_3, –CH_2– asym stretch), 2855 vs (–CH_2, CH_3 sym stretch), 1743 vs (–C=O ester stretch), 1464 s (–CH_2– deform), 1378 m (–CH_3 deform), 1244 m-s (O=C–C stretch), 1167 s (–O–C–C–), 1101 m-s (–CHO–), 725 w (–CH_2– wag).

Acetylated Milkweed Polyhydroxy Fatty Acids

MWPHFA (0.50 g, 0.48 mmol) were placed in a 50-mL flame-dried flask equipped with a magnetic stirrer. Acetic anhydride (4.0 mL, 42.62 mmol) and redistilled triethyl amine (0.2 mL) were added. The mixture was stirred and warmed to 55 °C for 4 h when reaction was complete. The product mixture was poured into saturated $NaHCO_3$ solution and stirred until effervescence ceased. The aqueous mixture was extracted with ethyl acetate (10 mL × 3) and the extract dried over Na_2SO_4 and concentrated at 57 °C to give the acetylated product, a viscous oil. FTIR spectrum film on NaCl disc ν cm^{-1}: 2928 vs (CH_3, CH_2 asym stretch), 2857 s (CH_3, CH_2 sym), 1740 vs (C=O ester), 1711 s (–CO_2 carboxyl), 1464 m (–CH_2– deform), 1373 s (–CH_3 deform), 1235 vs (O=C–C stretch), 1027 s (–CH_2O), 947 m (in-plain bend), 725 w(out-of-plain wag). The ^{1}H NMR ($CDCl_3$) δ (ppm): 2.42 t ($J = 7.4$ Hz, 7H), 2.04 s (22H), 1.6 m (14H), 1.45 m (13H), 1.21 bs (82H), 0.83 t ($J = 6.4$ Hz, 15H); ^{13}C NMR in $CDCl_3$ δ (ppm): 170.7, 170.6, 170.46, 170.3 (free –CO_2H groups); 169.4 (broad, acetyl groups); methine carbons bearing an oxygen atom—81.6, 81.55, 77.81, 75.14, 75.12, 74.92, 74.86, 74.43, 74.21, 73.76, 73.73; α- –CH_2– to carboxyls– 35.45, 35.19, 31.85, 31.75, 31.59; –CH_2s contiguous to methine carbons–30.67, 30.63, 30.60, 29.61, 29.58, 29.55, 29.31, 29.30, 29.28, 29.16, 29.14, 28.65, 25.02, 24.09, 24.06, 22.57, 22.41 ppm; the acetoxy methyl groups are at 21.03, 20.93, 20.92, 20.86 and 20.85 ppm; and the terminal methyl groups are at 14.05, 14.02, 13.96, 13.92, 13.91 ppm.

FTIR Spectroscopy

FTIR spectra were measured on an Arid Zone FTIR spectrometer (ABB Bomem MB-Series, Houston, TX, USA) equipped with a DTGS detector. Liquid derivatives were pressed between two NaCl discs (25 mm × 5 mm) to give thin transparent oil films for analysis by FTIR spectrometry. Absorbance spectra were acquired at 4 cm^{-1} resolution and signal-averaged over 32 scans. Interferograms were Fourier transformed using cosine apodization for optimum linear response. Spectra were baseline corrected, scaled for mass differences and normalized to the methylene peak at 2927 cm^{-1}.

Nuclear Magnetic Resonance: Distortionless Enhancement Proton Transfer

Nuclear magnetic resonance (NMR) spectra were acquired on an AV-500 MHz Spectrometer with dual 5 mm proton/carbon probe (Bruker, Ballerica, MA, USA). Distortionless enhancement proton transfer (DEPT) experiments were conducted in software provided with the Bruker Spectrometer.

Differential Scanning Calorimetry

Samples were analyzed using a Q2000 DSC (TA Instruments, New Castle, DE, USA). Each sample of MWPHFA (30–35 mg) was placed in a stainless steel pan and hermetically sealed. To eliminate their thermal history, the MWPHFA samples were loaded on the DSC and heated to 100 °C and cooled to −50 °C at rates from 3 to 15 °C/min, incrementing by 2 °C/min according to Ozawa crystallization kinetics [2]. After each cooling cycle, the samples were heated at 10 °C/min to 80 or 100 °C, and then cooled for the next heating rate. This cooling-heating method was repeated on each sample to ensure that no degradation occurred. Each sample was run in duplicate, where the onset peak temperatures and enthalpy of the crystallization peaks were recorded. For the kinetic analysis, the onset

and T_p were analyzed using the Ozawa [2] model to calculate E_a.

Thermogravimetric Analysis

TGA was performed using a 2050 TGA (TA Instruments, New Castle, DE, USA). For decomposition kinetic analysis, each sample (10–20 mg) was heated in a platinum pan under nitrogen atmosphere at three different heating rates: 10, 15, and 20 °C/min, for up to 800 °C. The data were analyzed using the TA Advantage Specialty Library software provided by TA Instruments (New Castle, DE, USA), which operates in accordance with ASTM E1641-07 Standard Test Method for Decomposition Kinetics by Thermogravimetry.

Pressure DSC (Oxidation Kinetics using Ozawa–Flynn–Wall Equation)

For pressure DSC, samples were analyzed on a 2920 DSC (TA Instruments, New Castle, DE, USA) using a pressure cell. Each sample (5–8 mg) was placed in a hermetically sealed pinhole aluminum pan for interaction of the sample with the reactant gas (oxygen). The sample was then sealed in the pressure cell chamber and prior to each run, the sample chamber was purged three times with oxygen. The sample was then run under an oxygen atmosphere at a pressure of 690 kPa (90 psi) with a purge rate of 150 mL/min from the outlet valve. These conditions maintain maximum contact with the sample and eliminate any limitation that might result from oxygen diffusion in the oil medium. However, extreme care was taken to maintain the pressure of the reactant gas (O_2) constant. The MWPHFA samples were first run at 5, 10, and 15 °C/min heating rates to 300 °C to determine the oxidation onset temperature (OT) and signal maximum temperature (SM). After determination of the OT for oxidation, each sample was then run using an isothermal method as follows: After purging the sample chamber, the run was started without oxygen to equilibrate at the isothermal temperature. After 4 min, oxygen was introduced to the sample and the temperature was held constant. The sample was allowed to run until the peak oxidation was reached.

The OT is defined as the temperature when a rapid increase in the rate of oxidation is observed in the system. This temperature is obtained by extrapolating the tangent drawn on the steepest slope of the reaction exotherm. A high OT would suggest a high oxidative stability of the sample, whereas a lower OT would indicate a thermally unstable sample. For kinetic studies, the inverse of the SM was plotted against the log of the heating rate. Using the linear regression method and subsequent data computation, various kinetic parameters were obtained.

Rheological Measurements

Rheological properties of MWPHFA samples were measured with a Rheometrics ARES strain-controlled fluids rheometer (TA Instruments, New Castle, DE) using an 8-mm diameter plate-plate geometry. The temperature was controlled at either 25 ± 0.1 or 50 ± 0.1 °C in the experiment chamber with a water circulation system. Prior to dynamic rheological parameter measurements, a strain-sweep experiment was conducted to ensure the experiments were conducted in a linear viscoelastic range. Linear viscoelasticity indicates that the measured parameters are independent of shear strains. Below 0.1% of strain, all measured materials in this study were in the linear range. Stress relaxation experiments were also performed in the linear viscoelastic range. These experiments measured the stress relaxation with time after the material was subjected to a step increase in strain. Small-amplitude oscillatory shear experiments (shear strain = 0.05%) were conducted over a frequency (ω) range of 0.1–500 rad/s, yielding the shear storage G' and loss G'' moduli. The storage modulus represents the non-dissipative component of mechanical properties. Elastic or "rubber-like" behavior is suggested if the G' spectrum is independent of frequency and greater than the loss modulus over a certain range of frequencies [5]. The loss modulus represents the dissipative component of the mechanical properties and is characteristic of viscous flow. The phase shift (δ) is defined by $\delta = \tan^{-1}(G''/G')$ and indicates whether a material is solid ($\delta = 0$), or liquid ($\delta = 90°$), or somewhere in between. Each measurement was repeated at least two times with different samples, where the relative errors were found to be within the range of ±10%.

Results and Discussion

MWPHFA were synthesized from the polyhydroxy triglyceride derivatives of milkweed oil [1] by saponification of the polyhydroxy triglyceride with KOH. Analysis of the FTIR spectrum of the isolated product indicated a material with different spectral characteristics from its triglyceride precursor, namely, the absence of the strong 1743 cm^{-1} ester carbonyl stretch of the parent now replaced by a 1714 cm^{-1} and a smaller 1558 cm^{-1} band corresponding to the –COOH and $–COO^-$, respectively, at pH 5.5. The presence of the 1558 cm^{-1} band indicated the need for a lower pH to complete protonation of the carboxylates (Fig. 1). Another characteristic difference in the FTIR spectra of MWPHTG and that of the free acid derivative, MWPHFA, is the change in frequency of the intense secondary hydroxyl –C–C–O stretch at 1175 cm^{-1} to that of the broad overlapping carboxylate O=C–C– stretch at

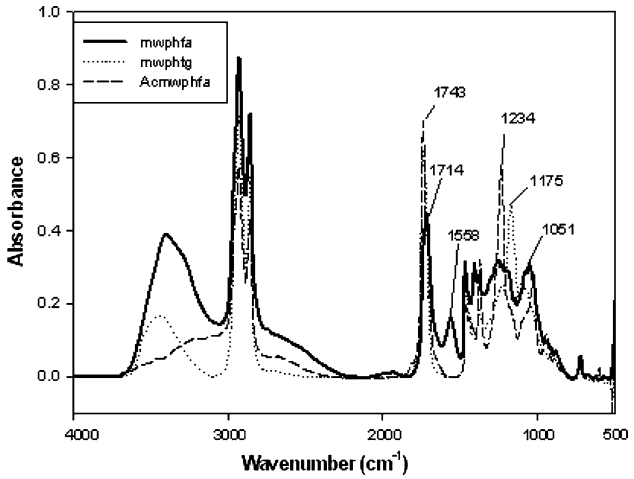

Fig. 1 FTIR spectra of MWPHFA, MWPHTG and AcMWPHFA

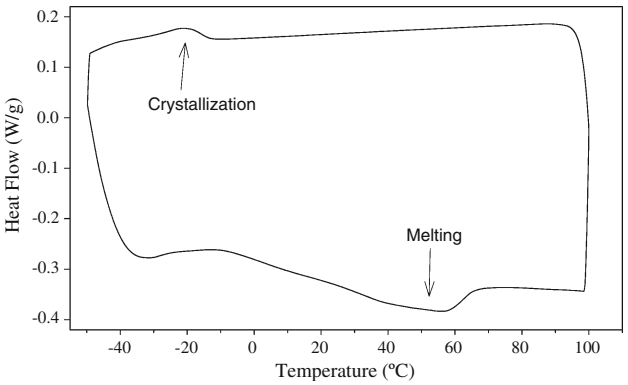

Fig. 2 DSC of MWPHFA (5 °C/min)

1234 cm^{-1}. Also is the noticeable drift in the spectral baseline in the 3600–2500 cm^{-1} region and the characteristic hump around 1980 cm^{-1}, a telltale of carboxylic acids. For the purpose of a cleaner and more definitive ^{1}H- and ^{13}C-NMR spectra of this product, the secondary hydroxyl moieties of MWPHFA were acetylated. The resulting ^{1}H-NMR spectrum of the ACMWPHFA showed five resonance envelopes of lines at 0.83, 1.45, 1.60, 2.04, and 2.39 ppm: the terminal methyl groups, most of the methylenes, the methyl groups of the acetyl substituents, and the methylene protons sandwiched between hydroxylated carbons, respectively. The terminal methyl groups of the acids naturally appeared as an overlapping triplet at 0.83 ppm with a J value of 6.4 Hz and integrate to 15 protons, whereas most of the methylenes show a broad multiplet centered at about 1.22 ppm and represents about 82 protons. There are two overlapping broad singlets centered around 1.5 ppm integrating respectively to 12 and 11 protons, whereas the methyl protons of the acetate are observed as an envelope of singlets centered at 2.04 ppm that integrate to some 22 protons. The resonance at 2.39 ppm is observed as a triplet integrating to 6 protons with a coupling constant of 6.4 Hz. This represents the C11 methylene protons of the linoleoyl species that are sandwiched between the methine protons of C10 and C12 of the acid. The main features of the ^{13}C were the free carboxyl resonances at 170.74, 170.62, 170.46, 170.41, and 170.39 ppm. The acetyl ester carbonyls show a single broad and intense resonance at 169.43 ppm, whereas the methine carbons appear at 81.63, 80.98, 77.81, 77.75, and 75.14–73.73 ppm. The methylene carbons appear as a major envelope of lines from 35.45 to 22.46 ppm; with the $–CH_2–$ α to the terminal carboxyls accounting for the resonances between 35.45 to 31.59 ppm and the methyl groups of the acetoxy substituents are observed at 21.03–20.86 ppm whereas the terminal methyl carbons of the acyl chains appear at 14.04–13.91 ppm. In addition both ^{1}H- and ^{13}C-spectra also revealed that the polyhydroxy triglyceride starting material retained a trace amount of unsaturation, a condition that the DSC experiment also hinted. The ^{13}C similarly confirmed the trace olefin with resonance lines barely above the spectral baseline at 135 and 124 ppm, respectively, and the DEPT experiment also indicated the presence of a trace amount of glycerol (64, 62 ppm for the –OCH– and $–CH_2O–$) in the sample.

MWPHFA samples were subjected to heating and cooling cycles using DSC. The cycling revealed a melting peak at 53.3 °C during heating and a crystallization peak at −21.5 °C at 5 °C/min heating rate. Evidently from Fig. 2, MWPHFA crystallized at a much lower temperature than that of its melting by 74 °C (53.3 + 21.5 °C), indicating variation in the molecular composition and structure. The ability of MWPHFA to re-crystallize following repeated heating and cooling cycling signifies a highly stable structure under the testing conditions. Higher heating rates resulted in a lower crystallization temperature (Table 1), where the ΔH was also decreased by higher heating rate. Although crystallization occurred at lower temperatures, evidently from the low ΔH a higher heating rate caused structural changes, permitting the molecules to crystallize more easily, Fig. 2. Similar behavior was noticed during rheological testing as will be discussed later. The crystallization kinetics of MWPHFA exhibited an E_a of 50.9 kJ as calculated using the T_p according to the data presented in Table 1 and as shown in Fig. 3. The E_a of MWPHFA crystallization was 70.6 kJ/mol when calculated from the basis of the OT. This is expected because the OT signifies the beginning of the crystallization process and it is closely connected to the heating rate, when the molecules still have some energy and are still mobile, unlike at the T_p when the crystallization process was complete.

The TGA scan of MWPHFA exhibited three degradation peaks at 271.7, 387.4 and 468.0 °C. Since the major

Table 1 Crystallization kinetics

Heating rate	T_o (°C)	T_p (°C)	T_o (K)	T_p (K)	$1/T_o$ (K) 10^{-3}	β/T_o^2 (10^{-6} min^{-1}/K^{-1})	$-\ln(\beta/T_o^2)$	$1/T_p$ (K) 10^{-3}	β/T_p^2 (10^{-6} min^{-1}/K^{-1})	$-\ln(\beta/T_p^2)$
3	−8.94 ± 0.23	−16.2 ± 0.63	264.4	257.5	3.78	42.92	10.06	3.88	45.26	10.00
5	−13.4 ± 0.14	−21.6 ± 0.63	259.9	252.1	3.85	74.05	9.51	3.97	78.70	9.45
7	−16.1 ± 0.21	−25.1 ± 0.56	257.3	248.6	3.89	105.78	9.15	4.02	113.31	9.09
9	−18.0 ± 0.14	−27.6 ± 0.49	255.3	245.9	3.92	138.14	8.89	4.07	148.78	8.81
11	−19.7 ± 0.21	−30.1 ± 0.49	253.7	243.5	3.94	170.97	8.67	4.11	185.60	8.59
13	−21.5 ± 0.21	−32.2 ± 0.49	252.2	241.4	3.97	204.47	8.50	4.14	223.18	8.41
15	−22.5 ± 0.14	−33.9 ± 0.49	250.8	239.6	3.99	238.57	8.34	4.17	261.40	8.25

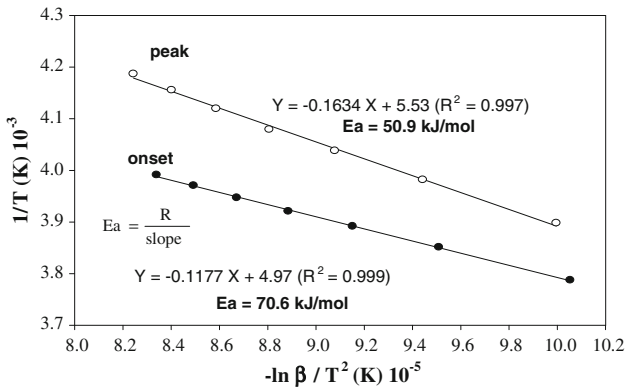

Fig. 3 DSC crystallization kinetics of MWPHFA (3–15 °C/min)

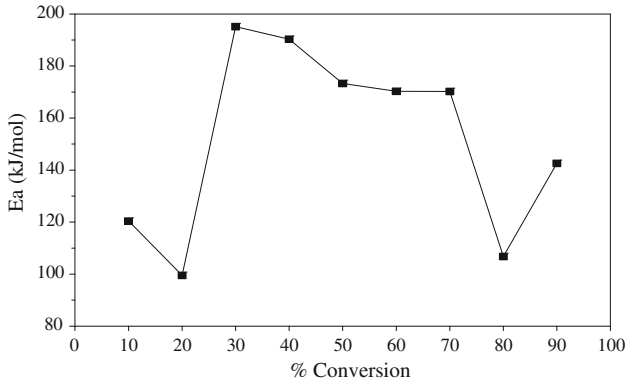

Fig. 4 TGA decomposition kinetics of MWPHFA

Table 2 Fatty acid composition of milkweed (*Asclepias syriaca*) oil[a]

Acid type	% Content
Oleic	31.0 (Δ^9, Δ^{11})
Linoleic	50.5
Linolenic	1.2
Palmitoleic	9.6 (Δ^9, $\Delta^{9,12}$)
Palmitic	5.7
Stearic	2.5

[a] From Ref. [1]

fatty acid composition of milkweed oil is linoleic, oleic and palmitoleic acids (Table 2), one can speculate that the three peaks seen on the TGA represent the three fatty acid types. The degradation E_a of the composite was calculated from the TGA data, where samples were heat-degraded in a nitrogen environment. The linear form of Ozawa–Flynn–Wall equation 3 was used for the calculation, where the slope of the line was the E_a. The equation was based on heating samples at different heating rates and the percent degradation-conversion of the material, in the form of weight loss, was determined and recorded after 10% of the material was degraded with a 10% increment. The degradation mechanism can be determined by plotting the E_a value as a function of percent degradation-conversion as shown in Fig. 4. It can be inferred from Fig. 4 that the degradation mechanism was a multi-step process reflecting the fatty acid composition of MWPHFA.

Since the pressure DSC measurements were performed in large excess of oxygen, the consumption of oxygen during the oxidation process can be neglected. This would also mean that, under this condition, the reaction rate is independent of the oxygen concentration and the reaction can be assumed to be first order as long as the oxidation initiation rate is constant. In a separate study, comparison of the peak areas or enthalpies for aged (ΔH_a) and fresh (ΔH_f) peanut oil confirms a first-order reaction for the oxidation process [6]. The OT shifts to a higher temperature with an increase in the heating rate (b) under constant oxygen pressure. The OT observed at each b was converted to the Kelvin values (absolute K) and its inverse was plotted against log b. Also, in earlier studies, the inverse of maximum heat flow temperature (K) of the MWPHFA sample exhibited Arrhenius behavior, as log of heating rate (b) varied linearly with the reciprocal of temperature (K) similar to what has been observed for other oil samples [7–9]. The slope of the line [$\delta \log b/\delta$ $(1/T)$] was generated from log b versus inverse temperature plot (Fig. 5) by a linear regression technique. A high coefficient of correlation ($R^2 = 0.99$) was obtained from the MWPHFA sample.

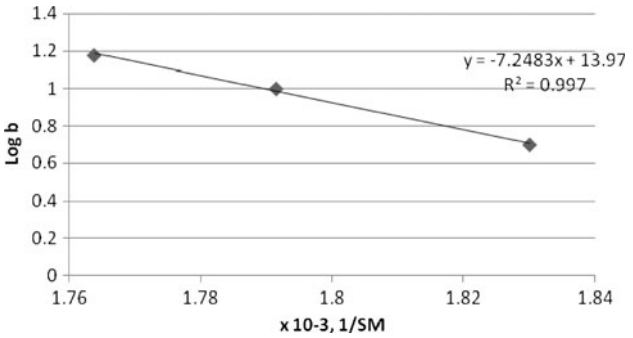

Fig. 5 Plot of inverse of SM (K) versus log b (heating rate)

Table 3 Calculated values of kinetic parameters of MWPHFA at a heating rate (b) of 10 °C/min

Kinetic parameters	Unmodified oil samples[a]	Milkweed PHFA
Activation energy (E_a, kJ/mol)	63–89	132
Maximum heat flow temperature (T, K)	454–477	558.2
E_a/RT	15.9–23.4	28.4
Arrhenius pre-exponential factor (Z)		1.14^{e12}
Ln Z	14.85–22.76	27.76
Specific rate constant (k, min^{-1})	0.33–0.51	0.51
Half life period ($t_{1/2}$)	1.36–2.07	1.36
Onset temperature (°C)	143–178	205

[a] Adhvaryu et al. [9]

Assuming a first-order reaction for the system during oxidation, the E_a and other kinetic parameters associated with the sample were calculated using the slope of the line (maximum heat flow temperature vs. heating rate) thus generated. The E_a was computed using the Ozawa–Flynn–Wall equation 4

$$E_a = -2.19R[\delta \log b/\delta(1/T)] \quad (4)$$

where b is the heating rate (°C/min) used. Since the reaction followed first-order kinetics, other kinetic parameters could be obtained from E_a for MWPHFA. The Arrhenius pre-exponential factor (Z) was calculated from E_a at a specific heating rate b using Eq. 5.

$$Z = (bE_a e^{E_a/RT})/(RT^2) \quad (5)$$

The temperature dependence of specific rate constant (k) can be described by Arrhenius equation 6.

$$k = Ze^{-E_a/RT} \quad (6)$$

And the half-life period can then be calculated using Eq. 7.

$$t_{1/2} = 0.693/k \quad (7)$$

Table 3 presents the calculated kinetic data of the MWPHFA obtained at heating rate (b) of 10 °C/min. It was observed that E_a for the MWPHFA was much higher

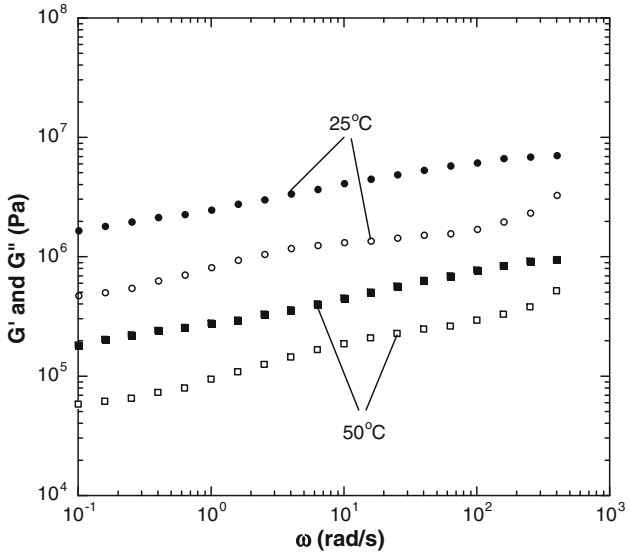

Fig. 6 Dynamic frequency-dependence moduli for MWPHFA at 25 and 50 °C. *Filled symbol G′*, *opened symbol G″*

compared to various unmodified oils [9], which varied in the range of 63–89 kJ/mol. This results in subsequent higher values of T, Z and k and much lower value of $t_{1/2}$. The extent of oxidation and formation of oxidation products are further complicated by the amount of unsaturation, methylene chain length and other functionalities present in the various triglyceride molecules [10]. The cumulative effect of all structural parameters in the triglyceride molecule makes oxidation a highly complex process and no simple kinetic model alone would hold for such systems.

In the case of unmodified vegetable oils, low poly-unsaturation, high mono-unsaturation, and high methylene content increases the E_a for oxidation. For MWPHFA, the E_a requirement is considerably high. This would result in delaying the onset of oxidation where bond scission takes place to form primary oxidation products, which is reflected in higher maximum heat flow temperature as well as higher OT. The absence of polyunsaturation explains the relative variation of E_a and other kinetic data between MWPHFA and unmodified vegetable oils.

Calculated values of E_a and k (Table 3) do not follow the theoretical inverse relation (E_a is directly proportional to inverse of k). The possible reason for this deviation is the large difference in the entropy of complex molecular structures that participate in oxidation reaction. Oxidation is a very complex process leading to numerous oxidation products involving various intermediates [11]. These intermediate compounds have their own k. The overall E_a is the cumulative effect of all the activation energies available in the system during the period of oxidation.

The linear rheological properties of dynamic frequency sweep results for MWPHFA at two temperatures are shown in Fig. 6. The stress relaxations after the MWPHFA

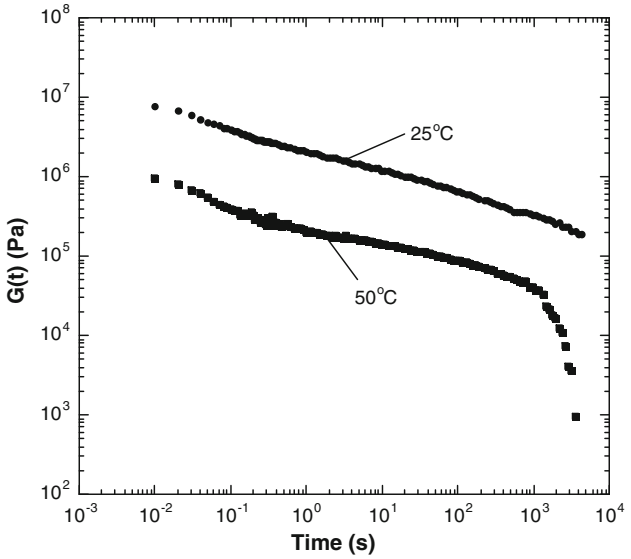

Fig. 7 Stress relaxation experiments for MWPHFA at 25 and 50 °C after the material was subject to an initial step shear strain of 0.05%

material was subjected to a step shear strain of 0.05% at two temperatures is shown in Fig. 7. At 25 °C, the MWPHFA material exhibited strong viscoelastic solid behavior where both storage moduli G' and loss moduli G'' were almost independent of frequency. The storage moduli G' were greater than the loss moduli within the whole range of the measured frequencies (Fig. 6). The G' values for MWPHFA at 25 °C were in the range of 1.7×10^6 to 7.2×10^6 Pa. The phase shift (δ) values were in the range of 15.5°–24.8°. These data are very comparable to the G' values for a highly cross-linked synthetic rubber which is around 10^7 Pa, and phase shift (δ) is about 11.5° at room temperature. Stress relaxation measurement showed that MWPHFA did not relax much after having been subjected to an initial shear strain for more than 4,000 s at 25 °C (Fig. 7). These results indicated that the MWPHFA exhibited strong viscoelastic solid properties like a strong gel or a weak rubber. Based on these findings, the MWPHFA material should have molecular structure comparable to an entangled network but not a chemically cross-linked network. If a network is tightly cross-linked chemically, there should not be any relaxation and relaxation time should be infinite. The MWPHFA material was observed to show stress relaxation with time, even though relaxation was very slow (Fig. 7), so there must be more of a physical chain–chain interaction rather than chemical ones within the MWPHFA network. Therefore, the reasonable explanation for the structure is that much stronger entanglements occur in MWPHFA that cannot quickly relax at room temperature. At 50 °C, MWPHFA still exhibited strong viscoelastic solid behavior, but was weaker than at 25 °C. Both storage moduli G' and loss moduli G'' were almost independent of frequency at 50 °C (Fig. 7). The G' values for MWPHFA at 50 °C were in the range of 4.7×10^5 to 3.3×10^6 Pa. The phase shift (δ) values were in the range of 16.6°–28.4°. At 50 °C, the MWPHFA material was weaker and slightly more fluid-like than it was at 25 °C as indicated by the lower G' value and greater phase shift. The stress relaxation measurement for the MWPHFA at 50 °C showed a very different result compared to the one at 25 °C (Fig. 7). The MWPHFA material did not relax a great deal until 1,300 s after it was subject to an initial step shear strain. However, after 1,300 s, the material relaxed very quickly (Fig. 7). These results implied that the MWPHFA network at 50 °C was not as strongly chain–chain entangled as it was at 25 °C. Therefore, the MWPHFA material can be considered as a network in which the chains can slip past each other for a relatively long time at 50 °C. The obtained rheological properties of MWPHFA above suggested that this material could have a potential usage in biodegradable plastics and gels for industrial and pharmaceutical applications.

Acknowledgments The authors express thanks to Dr. Karl Vermillion for the NMR data and Jason Adkins for technical assistance.

References

1. Harry-O'kuru RE, Holser RA, Abbott TP, Weisleder D (2002) Synthesis and characteristics of polyhydroxy triglycerides from milkweed oil. Ind Crops Prod 15(1):51–58
2. Ozawa T (1970) Kinetic analysis of derivate curves in thermal analysis. J Thermal Anal 2(3):301–324
3. Mohamed A, Gordon SH, Harry-O'kuru RE, Palmquist DE (2005) Phospholipids and wheat gluten blends: interaction and kinetics. J Cereal Sci 41(3):259–265
4. Flynn JH, Wall LA (1966) A quick direct method for the determination of activation energy from thermogravimetric data. Poly Lett 4(5):323–326
5. Ferry JD (1980) Viscoelastic properties of polymers, 3rd edn. Wiley, New York
6. Litwinienko G, Kasprzycka-Guttman T, Jarosz-Jarszewska M (1995) Dynamic and isothermal DSC investigation of the kinetics of thermooxidative decomposition of some edible oils. J Therm Anal Calorim 45(4):741–750
7. Litwinienko G, Daniluk A, Kasprzycka-Guttman T (1999) A differential scanning calorimetry study on the oxidation of C12–C18 saturated fatty acids and their esters. J Am Oil Chem Soc 76(6):655–657
8. Kowalski B (1995) Oxidative stabilities of engine oils contaminated by vegetable oil. Thermochim Acta 250(1):55–63
9. Adhvaryu A, Erhan SZ, Liu ZS, Perez JM (2000) Oxidation kinetic studies of oils derived from unmodified and genetically modified vegetables using pressurized differential scanning calorimetry and nuclear magnetic resonance spectroscopy. Thermochim Acta 364:87–97
10. Moll C, Biermann U, Grosch W (1979) Occurrence and formation of bitter-tasting trihydroxy fatty acids in soybeans. J Agric Food Chem 27(2):239–243
11. Tian K, Dasgupta PK (1999) Determination of oxidative stability of oils and fats. Anal Chem 71(9):1692–1698